

Stair Climbing Control of 4-Degrees-of-Freedom Tracked Vehicle Based on Internal Sensors

Daisuke Endo

Atsushi Watanabe

Keiji Nagatani

Tohoku University, endo@frl.mech.tohoku.ac.jp Tohoku University, atsushi.w@ieee.org Tohoku University, keiji@ieee.org

Abstract—In search and rescue missions, multi-degree-of-freedom (DOF) tracked robots that are equipped with subtracks are supposed to be useful. These types of robots have superior locomotion performance on rough terrain. However, in teleoperated missions, the performance of tracked robots relies on the operators' skill to control every subtrack appropriately. Therefore, an autonomous traversal function can significantly help in the teleoperation of such robots. In this paper, we propose a planning and control method for 4-DOF tracked robots traversing known stairs automatically, based on internal sensors.

Some experimental results in mock-up stairs verify the effectiveness of the proposed method.

I. INTRODUCTION

In search and rescue missions, it is widely known that multi-degrees-of-freedom (DOF) tracked robots that are equipped with subtracks are very useful. Quince is a typical example of such a multi-DOF tracked robot. It explored buildings affected by the meltdown accident in the Fukushima Daiichi nuclear power plant [1][2]. Such a multi-DOF tracked robot has main tracks that constitute a skid-steered mobile base, and each one rotates independently. In addition, it is equipped with subtracks that connect to the main body with rotary joints at the front and rear of the main tracks. It has high traversability on rough terrains in spite of its relatively simple mechanism.

In the case of search and rescue missions, a tracked vehicle is sometimes required to traverse stairs to go to another floor and expand the reachable area. However, stairs represent typical uneven ground, and are likely to cause some trouble for ground vehicles, even if it is a multi-DOF tracked robot. Particularly, if its sub-tracks are operated inadequately, it can cause fatal failure modes, such as tipping over. Moreover, in teleoperated missions, the operation of the subtracks is a difficult task and can easily cause operation errors. Therefore, it requires sophisticated operator skills.

To solve this problem, Okada et al. realized a shared autonomous system to control subtracks adaptively by mounting laser range sensors on the multi-DOF tracked robot to detect the ground shape under the robot body [3]. Li et al. developed an autonomous system to traverse stairs by using Kinect sensor [4]. As mentioned in each paper, these are effective systems. However, each approach requires dedicated external sensors to detect the shape of the stairs. In addition, Ohno et al. proposed a semi-autonomous approach to make the subtracks stay in contact with the unknown shape ground by realizing compliant joints based on joint torque information [5]. However, this approach requires a current sensor on each

subtrack to obtain the joint torque, and the sensor information is affected by the friction of its transmissions. To reduce the effect of the friction, the reduction ratio of the gear should be small. However, the essential power of subtracks to control on uneven terrain is limited. The above conventional approaches are primarily for unknown natural rough terrain. On the other hand, there are some cases where the shape of the stairs is known, and in such simple cases, the robot does not require external sensors. Therefore, in this paper, we propose an autonomous motion for a 4-DOF tracked robot to traverse known stairs based on the rotational velocity of the main tracks, the rotational position of the subtracks, and IMU (Inertial Measurement Unit) information, without any other external and internal sensors. Besides, some conventional multi-DOF tracked robots, for example Quince, are 6-DOF, which has four subtracks, one each at the front-left, front-right, rear-left, and rear-right of the main tracks. However, in the case of typical climbing/descending of stairs, the left and right subtracks are not operated independently but synchronized. Therefore, our proposal is also useful for 6-DOF tracked robots. In addition, some verification tests are reported to confirm the validity of the proposed method.

II. PROBLEM DESCRIPTION

Our goal of this research is to realize an autonomous motion for a 4-DOF tracked robot to traverse known stairs based on the rotational velocity of the main tracks, the rotational position of the subtracks, and IMU information. The target robots and target environments are described in the following.

A. Target robot

In this research, we deal with 4-DOF tracked robot. It consists of two main tracks to enable skid steering. It has two sets of two synchronous subtracks. One pair is on both sides of the front, and the other is on both sides of the rear. The rotation range of each subtrack is more than $\pm 90^\circ$ with respect to the front-rear direction of the main tracks. In addition, there are multiple grousers on the periphery of each track to improve friction between the track and the ground. These should be enough to prevent the robot from slipping down. We assume that the rotation counts of the main tracks and the subtracks are obtained by internal sensors, such as rotary encoders, which enables odometry. The robot's pose is obtained by an IMU that contains acceleration sensors and gyroscopes. The definition of each specification parameter is described in Fig. 1-(i).

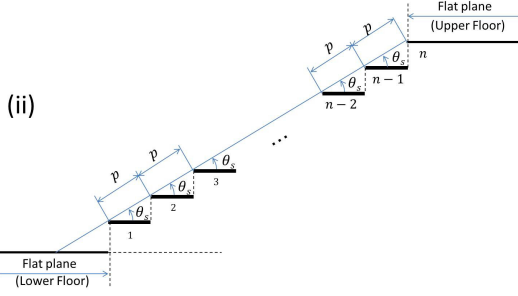
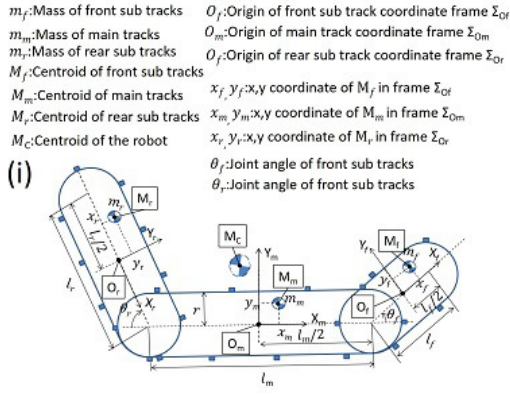


Fig. 1. Assumed shape of the robot and the stairs

B. Target environment

In this paper, we deal with an environment that consists of two different horizontal floors that are connected by stairs, with all steps in parallel. The distance (pitch) p and inclination θ_s between two adjacent edges of the stairs are constant.

We assume that all steps have a horizontal plane, and the existence of a vertical plane is arbitrary. p , θ_s , and the number of steps n are known. The width of the stairs is sufficiently larger than that of the robot. In addition, we assume that the relationship between p and the maximum length of flat area under the robot $L = l_f + l_m + l_r$ is $L \geq 2p$. This assumption means that the robot can traverse the stairs while maintaining an inclination of the robot that is equal to that of the stairs. In addition, the conditions of (p, θ_s) are limited in that falling backward (described later) does not occur in the case the robot stretches all subtracks completely straight. This assumption physically means that the robot at least has a way to traverse the stairs.

III. DEFINITIONS OF PHASES OF TRAVERSING MOTION AND FAILURE MODES

While a tracked robot traverses the stairs, there are roughly three phases of the motion (shown in Fig. 2), and each phase has different characteristic problems. In this section, we describe the definitions of the three phases and the problems that tend to occur in each phase.

A. Definition of the three phases of the traversing motion

First, we divide the stair climbing motion into three phases, as follows:

(i) Pitch-up phase:

The phase starts when the robot touches the first step

--- Trajectory of a representative position of the robot

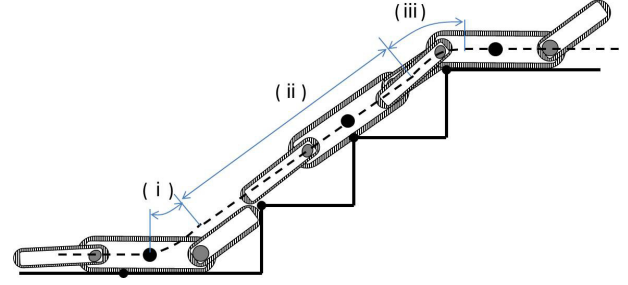


Fig. 2. Three phases of traversing stairs

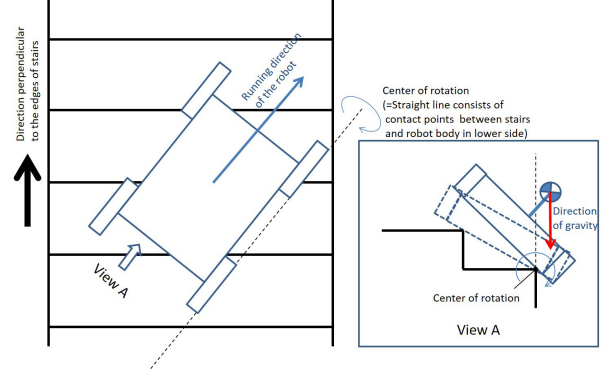


Fig. 3. Falling sideward

of the stairs and lasts until the inclination of the robot corresponds to that of stairs (Fig. 2-(i))

(ii) Normal climbing phase:

The phase between (i) and (iii). During this phase, the inclination angle of the robot is equal to that of the stairs (Fig. 2-(ii)).

(iii) Pitch-down phase:

The phase during which the inclination angle of the robot starts decreasing and leads to the robot successfully reaching the new level (Fig. 2-(iii)).

B. Definition of the failure modes

While the robot traverses the stairs, it is necessary to prevent the following four failure modes:

1) Slipping mode:

The friction between the tracks and the steps is not sufficient to move the robot forward.

2) Falling backward:

The robot body rotates backward and downward around the lowermost contact point to the stairs (flips over backwards).

3) Falling sideward:

The robot body rotates sideward around the axis of the contact line of the robot's side (tips sideways as shown in Fig. 3).

4) Excessive shock:

The contact shock exceeds the acceptable level for the robot (or surrounding environment) when it climbs over the final step of the stairs (as shown in Fig. 4).

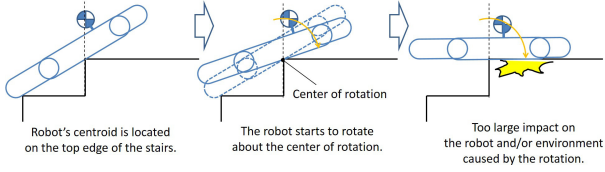


Fig. 4. Excessive shock

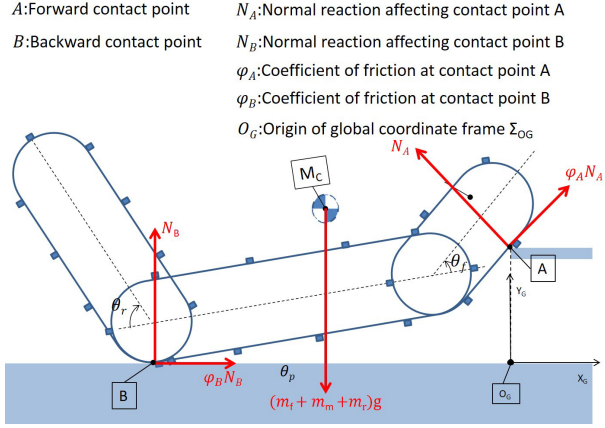


Fig. 5. Physical model in the pitch-up phase

IV. MOTION STRATEGY

The occurrence of the failure modes depends on the motion phases described in the previous section. In this section, we describe the failure modes that easily occur in each phase, and a motion strategy to prevent these failure modes.

A. Slip prevention in pitch-up phase

A failure that easily occurs in the pitch-up phase is slippage between the tracks and the ground that consists of the stairs and the lower floor. Thus, the motion of the robot should be pre-determined in advance to prevent the slipping mode. For this reason, it is desirable that the reference joint angles of the subtracks θ_f and θ_r are set to increase friction. According to Yugang et al., when a tracked robot with grousers makes contact at the peak of a step, as shown in Fig. 5, the equivalent friction coefficient (the value calculated from the force affecting in peripheral direction divided by the force affecting in normal direction) at the contact point A φ_A can be calculated by [8]:

$$\varphi_A = \frac{\sin(\theta_f + \theta_p) + \mu \cos(\theta_f + \theta_p)}{\cos(\theta_f + \theta_p) - \mu \sin(\theta_f + \theta_p)}, \quad (1)$$

where μ is the friction coefficient between the materials of the grousers and the materials of the stairs. Therefore, the friction of the front subtrack is maximized when the denominator on the right side of Eq. (1) is equal to zero. Hence, the slipping mode can be minimized when the reference angle of the front subtrack θ_f^{ref} is determined as:

$$\theta_f^{ref} = \arctan\left(\frac{1}{\mu}\right) - \theta_p. \quad (2)$$

Incidentally, φ_A equals to infinity in this condition mathematically. It means that finite force affects on the contact point A even if the normal force equals to zero by hooking of the grousers actually. In addition, in case the robot lifts up its main body from the horizontal state, the friction coefficient necessary to rise up the body becomes smaller as the front contacting point comes closer to the rear contacting point [9].

On the other hand, to prevent the falling backward mode, it is desirable that the rear subtracks stay very close to the ground to prevent from falling backward. Based on the above, we can conclude that the reference joint angle of the rear subtrack θ_r^{ref} is determined as follows:

$$\theta_r^{ref} = \theta_p + \delta, \quad (3)$$

where δ is the margin of the rear subtrack not to contact to the lower floor, even if any error or delay of control occurs.

B. Falling backward and sideward prevention in normal climbing phase

In normal climbing phase, two falling modes, falling backward and falling sideward, easily occur. It is possible to prevent the falling backward mode when the subtracks are operated properly. On the other hand, it is difficult to escape from the falling sideward mode in case that the robot's orientation differs from the vertical direction to the edges of the stairs, even if subtracks are operated properly. Control methods to prevent from the above two failure modes are described in the following subsections.

1) *Prevention of Falling backward by using subtracks:* The falling backward mode occurs in case that zero moment point of the robot moves downward, and gets out of the range of the support polygon. Thus, when the robot climbs stairs, it is desirable that the centroid is located as low and frontward as possible, and also extend the support polygon backward. Based on the above, it is effective that the front subtrack is extended frontward, and the rear subtrack is extended backward to locate all contact points in one flat plane. Hence, the reference joint angles of the subtracks in the normal climbing phase are described below by Eqs. (4) and (5).

$$\theta_f^{ref} = 0 \quad (4)$$

$$\theta_r^{ref} = 0 \quad (5)$$

2) *prevention of Falling sideward by using main tracks:* To prevent from falling sideward, it is desirable that the orientation of the robot matches the vertical direction of the stairs as closely as possible. Therefore, it is effective that main tracks are controlled based on a control law of Eq. (6) by using ϕ , which is the angle between the orientation of the robot and the direction of the stairs:

$$\Omega^{ref} = -k_\phi \phi, \quad (6)$$

where Ω^{ref} is the target angular velocity of the robot body, and k_ϕ is the control gain. The problem is how to detect ϕ . In our assumption, the robot does not have any external sensors. Furthermore, in case that the left and the right main

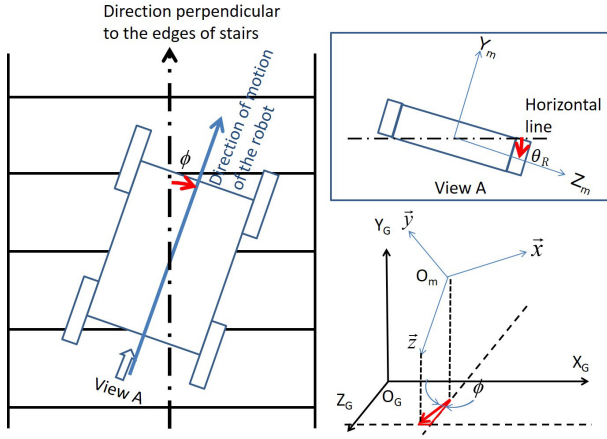


Fig. 6. Vertical climbing direction and orientation of the robot

tracks slipped unequally on the stairs, and the yaw angle of the robot obtained by a gyroscope may drift. This causes an increase in the estimation error of ϕ when the robot relies on some dead reckoning method like odometry or its gyroscope only. Therefore, to solve this problem, we propose a method to calculate ϕ based on the roll information on gravity direction. Let \vec{z} be a unit vector pointing to the left of the robot body in the Σ_G coordinate system, and \vec{t} a unit vector in the direction perpendicular to the edges of the stairs in the Σ_G coordinate system (Fig.6). As $\vec{z} \cdot \vec{t} = \cos(\frac{\pi}{2} - \phi)$, we can derive:

$$\phi = \frac{\pi}{2} - \arccos\left(\frac{\sin \theta_s \sin \theta_R}{1 - \cos \theta_s \cos \theta_R}\right), \quad (7)$$

where θ_R is the roll angle of the robot body with respect to the gravity direction. Equation (7) indicates that ϕ can be obtained from the inclination of the stairs θ_s and the roll angle of the robot body θ_R . θ_s is also known and θ_R can be detected by an internal sensor only, IMU, without drift. Besides, the switch of control law from the pitch-up phase to the normal climbing phase is conducted when the pitch angle of the robot body θ_p comes sufficiently close to the inclination of stairs θ_s . Specifically, the control law is changed when the condition

$$\theta_p \geq \theta_s - e_p, \quad (8)$$

is established. Here $\pm e_p$ describes the detection error range of the pitch angle of the robot.

C. Shock mitigation in pitch down phase

In the pitch-down phase, the robot should be most careful to mitigate the shock affected between the robot body and the ground when it touches down on the upper floor. For shock mitigation, the ideal of a soft landing motion makes the height of free fall equal to zero. This motion can be created theoretically by making the front subtrack make contact to the upper floor just before the centroid projection point of the robot body passes the peak of the final step. It can be realized only when the position of the robot is estimated without error. However, it is difficult for the robot to keep the accuracy of

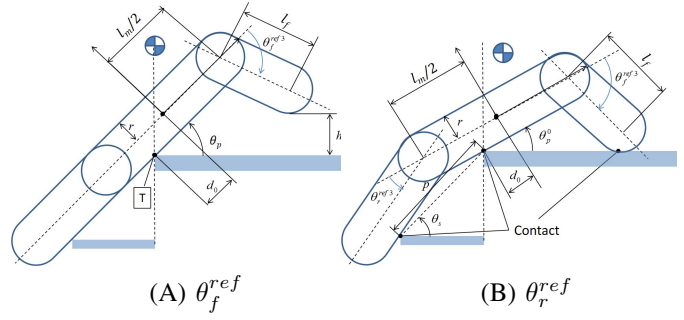


Fig. 7. Target angle of subtracks in pitch down mode

the position estimation at high quality on stairs where it tends to experience slip or oscillation.

In case the front subtracks contact the upper floor with the robot's position estimation error, it may hit the peak of the final step or the upper floor strongly. As a result, θ_p increases, and in the worst case, the falling backward mode occurs. To avoid the above situation, in this paper, we propose a method that absorbs the position estimation error for practical use. Specifically, the robot operates in a motion such that its height of free fall does not exceed the maximum acceptable height h_{max} for the robot and the surrounding environment when the robot touches down on the upper floor.

Fig. 7-(A) indicates a state where the joint angles of the rear subtracks are equal to zero, and the zero moment point matches the peak of the final step. This is the state transition configuration for which the robot starts to fall down forward, and h indicates the height of free fall. Based on the geometric condition of Fig. 7-(A), the reference joint angle of the front subtrack should be θ_f^{ref} , described in Eq. (9) below, to make the height of free fall equal to the intended h less than h_{max} .

$$\theta_f^{ref} = \arcsin\left(\frac{\frac{l_m}{2} \sin \theta_s - r(1 - \cos \theta_s) - h - d_0 \sin \theta_s}{l_f - \theta_s}\right), \quad (9)$$

where d_0 is the offset distance in the front-back direction of the robot between the peak of the final step and the center of the main tracks, as shown in Fig. 7-(A).

On the other hand, the joints of the rear subtracks should be controlled downward slightly, to support the robot body falling forward smoothly, as shown in Fig. 7-(B). A suitable angle of the rear subtrack can be determined by the configuration of the robot in the figure: the three contact points do not generate the internal force to grasp the stairs.

Depending on the geometric condition, the reference joint angle of the rear subtrack θ_r^{ref} can be calculated by :

$$\theta_r^{ref} = \arctan\left(\frac{p \sin \theta_s - (l_m/2 + d_0) \sin \theta_p^0}{p \cos \theta_s - (l_m/2 + d_0) \cos \theta_p^0} - \theta_p^0\right), \quad (10)$$

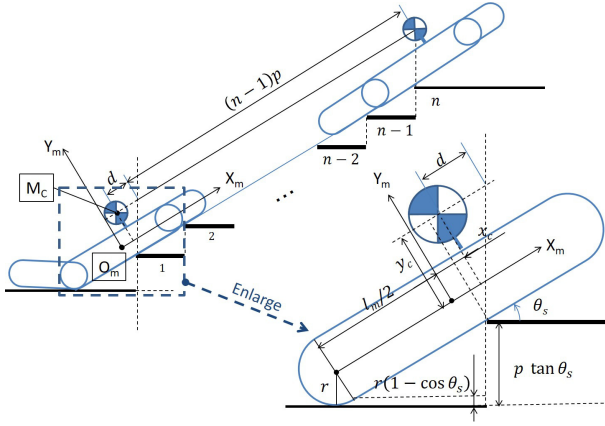


Fig. 8. Distance to move in the normal climbing phase

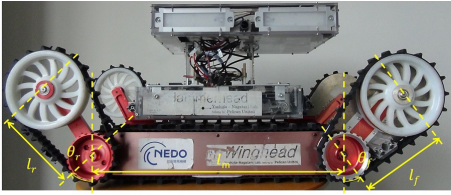


Fig. 9. The tracked robot used in tests

where θ_p^0 is the pitch angle of the robot body when the front subtrack makes contact with the upper floor after the robot falls down forward. Thus, it satisfies

$$\left(\frac{l_m}{2} - t_0\right) \sin \theta_p^0 + r \cos \theta_p^0 - l_f \sin(\theta_f - \theta_p^0) - r = 0. \quad (11)$$

As we assume that the robot has no external sensors in this research, the phase transition from the normal climbing phase to the pitch down phase is conducted when its running distance D in the normal climbing phase exceeds a fixed value, as shown in the following Equation:

$$D \geq d + (n - 1)p, \quad (12)$$

where n is the number of steps. d is a dimension indicated in Fig. 8, which according to the geometric condition is determined by

$$d = (r + y_c) \tan \theta_s + \frac{p \tan \theta_s - r(1 - \cos \theta_s)}{\sin \theta_s} - \frac{l_m}{2} - x_c. \quad (13)$$

V. VERIFICATION TEST

We verified our proposed method described in the previous section by conducting tests with a tracked robot on mock-up stairs. In this section, the procedures, results, and discussion of these verification tests are described.



Fig. 10. Changeable mock-up stairs

A. Test equipment

1) *Tracked robot*: We used the tracked robot Kenaf [6][7] in our laboratory for verification tests (Fig. 9). The Kenaf is a 6-DOF tracked robot: two main tracks for traversal, and four subtracks, which are located on both sides at the front and rear of the robot, and can be controlled independently. However, left and right subtracks are synchronized in the verification tests. Table I indicates the parameters of the Kenaf.

Incidentally, the shape of the Kenaf projected from the side is different from Fig. 1. That is because the diameters of the outer pulleys of the subtracks are larger than that of the semicircular parts of the main tracks. However, according to Fig. 9, each Kenaf's parameter, such as l_f , l_m , and l_r , is equivalent with our proposed model as shown in Table I.

In addition, the robot has a 9-axes IMU sensor module RT-USB-9AXIS-00 made by RT Co., Ltd. on the main tracks to detect the pitch and roll angles of the robot with respect to the gravity direction.

2) *Mock-up stairs*: The pitch p and inclination θ_s between two adjacent edges of the stairs are constant. To confirm the proposed method, we use mock-up stairs, as shown in Fig. 10. It can change both the pitch p between two adjacent edges of the stairs, and its inclination θ_s . θ_s can be changed from 0 to 70°, and p can be changed to any value up to 2400 mm.

TABLE I
SPECIFICATION OF THE ROBOT
(MT:MAIN TRACKS, ST:SUBTRACKS)

Parameter	Symbol	Value
Length of flat area in front ST	l_f	155[mm]
Length of flat area in MT	l_m	470[mm]
Length of flat area in rear ST	l_r	155[mm]
Radius of circular part in MT	r	56[mm]
Mass of front ST	m_f	2.1[kg]
Mass of MT	m_m	22.8[kg]
Mass of rear ST	m_r	1.6[kg]
Centroid of front ST(x in frame Σ_{O_f})	x_f	15[mm]
Centroid of front ST(y in frame Σ_{O_f})	y_f	15[mm]
Centroid of MT(x in frame Σ_{O_m})	x_m	0[mm]
Centroid of MT(y in frame Σ_{O_m})	y_m	45[mm]
Centroid of rear ST(x in frame Σ_{O_r})	x_r	-10[mm]
Centroid of rear ST(y in frame Σ_{O_r})	y_r	16[mm]

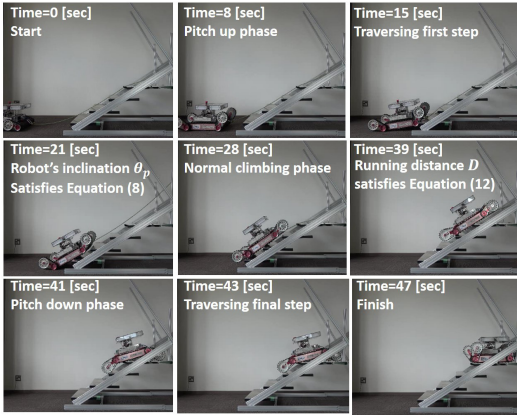


Fig. 11. Behavior of the robot for $\theta_s = 30^\circ$, $p = 300$ mm

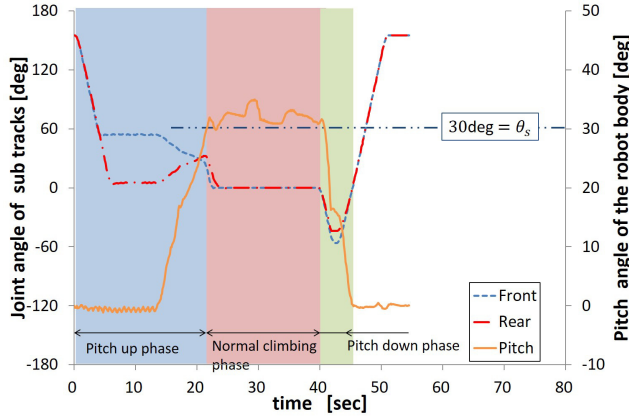


Fig. 12. Data profile of θ_f , θ_r , and θ_p ($\theta_s = 30^\circ$, $p = 300$ mm)

B. Test procedure

We implemented the proposed method on the Kenaf, and conducted traversal tests on the mock-up stairs with a safety lope in front of the robot. Running speed of the main tracks was set at 5 cm/s. For Eqs. (1) and (2), we set the friction coefficient to $\mu = 0.74[-]$ based on our preliminary test. The margin of the rear subtrack not to contact the lower floor was set as $\delta = 6^\circ$. The height of the free fall margin h was set at 50 mm for the condition $\theta_s = 30^\circ$, and 80 mm For $\theta_s = 45^\circ$. According to some preliminary experiments, the detection error of the pitch angle of the robot body was $e_p = 2.9^\circ$.

Based on the above parameters, we conducted verification tests under three different conditions: $(\theta_s, p) = (30^\circ, 200$ mm), $(30^\circ, 300$ mm), and $(45^\circ, 200$ mm), and with three trials for each condition. The number of steps $n = 4$.

C. Test results

The Kenaf traversed the mock-up stairs in all conditions without any failure modes. Figs. 11 and 12 indicate a behavior and profiles of θ_p , θ_f , θ_r , and the motion phase, respectively, for $(\theta_s, p) = (30^\circ, 300$ mm). According to Fig. 12, the motion phases transitioned appropriately, and the pitch angle of the robot body matched the inclination of the stairs. Consequently,

the proposed method was applied to various cases in different configurations of stairs.

VI. CONCLUSION

In this paper, we described a method to make a 4-DOF tracked robot traverse known stairs based on internal sensors, autonomously. We classified three motion phases and four failure modes while the robot traverse the stairs, and then proposed an effective motion in each phase to prevent failure modes. Moreover, the transitions from one phase to the next are also realized based mainly on the inclination sensor of the robot body. As a results of the verification tests, we confirmed that a 4-DOF tracked robot traversed the stairs without any failure modes based on our proposed method.

In future work, we expect that the method can be expanded to more difficult situation such that the shapes of stairs are unknown, by utilizing external sensors effectively.

ACKNOWLEDGMENT

This work was supported in part by the ARGOS challenge organized by TOTAL Co., Ltd. and a Grant-in-Aid for JSPS Fellows (No.16J2554). We would like to thank Editage (www.editage.jp) for English language editing.

REFERENCES

- [1] Tomoaki Yoshida, Keiji Nagatani, Satoshi Tadokoro, Takeshi Nishimura, and Eiji Koyanagi. Improvements to the rescue robot Quince toward future indoor surveillance missions in the Fukushima Daiichi Nuclear Power Plant. Preprints of the 8th International Conference on Field and Service Robotics, #80, 2012.
- [2] Keiji Nagatani, Seiga Kiribayashi, Yoshito Okada, Satoshi Tadokoro, Takeshi Nishimura, Tomoaki Yoshida, Eiji Koyanagi, and Yasushi Hada. "Redesign of rescue mobile robot Quince -Toward emergency response to the nuclear accident at Fukushima Daiichi Nuclear Power Station on March 2011-", Proceedings of the 2011 IEEE Int'l Workshop on Safety, Security and Rescue Robotics, pp.13-18 (2011-11)
- [3] Yoshito Okada, Keiji Nagatani, Kazuya Yoshida, Tomoaki Yoshida, and Eiji Koyanagi. Shared autonomy system for tracked vehicles to traverse rough terrain based on continuous three-dimensional terrain scanning. 2010 IEEE/RSJ International Conference on Intelligent Robots and Systems, pages 357-362, 2010.
- [4] I-Hsum Li, Wei-Yen Wang, and Chien-Kai Tseng. A Kinect-sensor-based Tracked Robot for Exploring and Climbing Stairs. International Journal of Advanced Robotic Systems 11, DOI: 10.5772/58583, 2014.
- [5] Kazunori Ohno, Shouichi Morimura, Satoshi Tadokoro, Eiji Koyanagi, and Tomoaki Yoshida. Semi-autonomous Control System of Rescue Crawler Robot Having Flippers for Getting Over Unknown-Steps. Proceedings of the 2007 IEEE/RSJ International Conference on Intelligent Robots and Systems, pages 3012-3018, 2007.
- [6] Tomoaki Yoshida, Eiji Koyanagi, Satoshi Tadokoro, Kazuya Yoshida, Keiji Nagatani, Kazuhro Ohno, Takashi Tsubouchi, Shoichi Maeyama, Itsuki Noda, Osamu Takizawa, and Yasushi Hada. A High Mobility 6-Crawler Mobile Robot 'Kenaf'. Proc. 4th International Workshop on Synthetic Simulation and Robotics to Mitigate Earthquake Disaster. page 38, 2007.
- [7] Kazunori Ohno, Satoshi Tadokoro, Keiji Nagatani, Eiji Koyanagi, and Tomoaki Yoshida. Trials of 3D Map construction using the tele-operated tracked vehicle Kenaf at Disaster City. 2010 IEEE International Conference on Robotics and Automation, pages 2864-2870, 2010.
- [8] Yungang Liu and Guangjun Liu. Track-stair Interaction Analysis and Online Tipover Prediction for a Self-Reconfigurable Tracked Mobile Robot Climbing Stairs. IEEE/ASE Transactions on Mechatronics, Vol. 14, No. 5., pages 528-538, 2009.
- [9] Jingguo Liu, Yuechao Wang, Shungen Ma, and Bin Li. Analysis of Stairs-Climbing Ability for a Tracked Reconfigurable Modular Robot. Proceedings of the 2005 IEEE International Workshop on Safety, Security and Rescue Robotics, pages 36-40, 2005.